ChemComm

Accepted Manuscript

This article can be cited before page numbers have been issued, to do this please use: X. Zhang, X. Hao, J. Yu, M. Zhou, J. Jie, C. Yu and X. Zhang, *Chem. Commun.*, 2013, DOI: 10.1039/C3CC47961G.

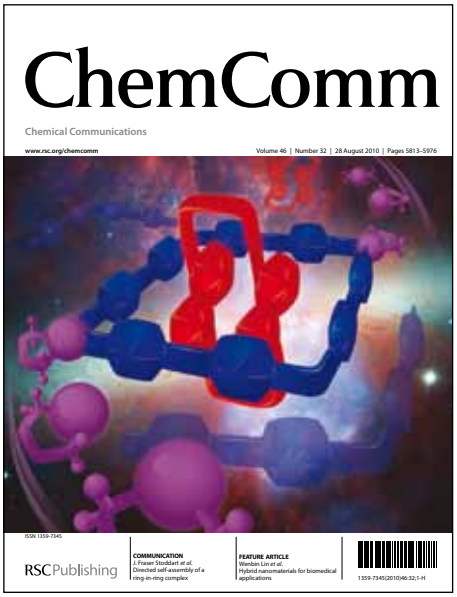

This is an *Accepted Manuscript*, which has been through the RSC Publishing peer review process and has been accepted for publication.

Accepted Manuscripts are published online shortly after acceptance, which is prior to technical editing, formatting and proof reading. This free service from RSC Publishing allows authors to make their results available to the community, in citable form, before publication of the edited article. This *Accepted Manuscript* will be replaced by the edited and formatted *Advance Article* as soon as this is available.

To cite this manuscript please use its permanent Digital Object Identifier (DOI®), which is identical for all formats of publication.

More information about *Accepted Manuscripts* can be found in the **Information for Authors**.

Please note that technical editing may introduce minor changes to the text and/or graphics contained in the manuscript submitted by the author(s) which may alter content, and that the standard **Terms & Conditions** and the **ethical guidelines** that apply to the journal are still applicable. In no event shall the RSC be held responsible for any errors or omissions in these *Accepted Manuscript* manuscripts or any consequences arising from the use of any information contained in them.

Cite this: DOI: 10.1039/c0xx00000x

www.rsc.org/xxxxxx

View Article Online
DOI: 10.1039/C3CC47961G

COMMUNICATION

High luminescent and photostable core/shell dye nanoparticles for high efficency bioimaging

Xiaojun Hao,[a] Mengjiao Zhou[a], Xiujuan Zhang,*[a] Jia Yu[a], Jiansheng Jie,*[a] Caitong Yu,[a] Xiaohong Zhang*[b]

Received (in XXX, XXX) Xth XXXXXXXXX 20XX, Accepted Xth XXXXXXXXX 20XX
DOI: 10.1039/b000000x

We developed core/shell silica-coated dye nanoparticles as highly bright and ultrastable red-emitting fluorescent probe for long-term cellular imaging and ultrasensitive in vivo animal imaging.

In vivo near-infrared (NIR) fluorescence imaging technique is highly desirable for sensitive cancer early detection, because biological tissues show very low absorption and autofluorescence in the NIR spectrum window.[1] Although quantum dots (QDs) have been widely explored for in vivo NIR imaging, their clearance from the physiological systems and the possible release of cytotoxicity heavy metals to biological systems is still a matter of concern. Organic dyes are still the most widely used fluorescent markers for NIR biological imaging, which are usually covalently linked or physically entrapped in various nanovehicles to improve their water dispersibility and bioenvironmental stability for bioimaging.[2] Recently, special dyes with the characteristics of aggregation-induced emission enhancement (AIEE) have attracted much attention, because they can achieve strong fluorescence when they are aggregated.[3] Especially, when they are made into dye nanoparticles (NPs), due to the remarkably enhanced absorptivity and fluorescence quantum yield (QY), the NPs can exhibit much improved brightness than that loaded in nanovehicles.[4] However, the dye NPs with enhanced emissions still suffer from the problems like (1) emission efficiency can be strongly affected by the external environment; (2) Surface properties still need to be improved to offer robust photostability for long-term imaging.

Silica is a good noncytotoxic and biocompatible material, it is expected that integration of dye NPs with silica shell to form core-shell structure will endow the nanocomposites with superior properties.[5] First, the silica shell can serve as a protective layer to isolate dye NPs from the external environment, which will effectively prevent unexpected quenching caused by the external surface adsorbates or redoxactive molecules. Second, silica shell is optically transparent and chemically inert in protecting the surface of the NPs from photobleaching by light. Third, silica surfaces are more easily to be functionalized by thiol, amine, and carboxylate groups to facilitate dye NPs for more versatile biological applications. Herein, we developed silica-coated dye NPs as highly bright and photostable NIR fluorescent probe for long-term cellular imaging and ultrasensitive in vivo animal imaging. Systematic in vivo toxicity study also demonstrated their favorable biocompatibility.

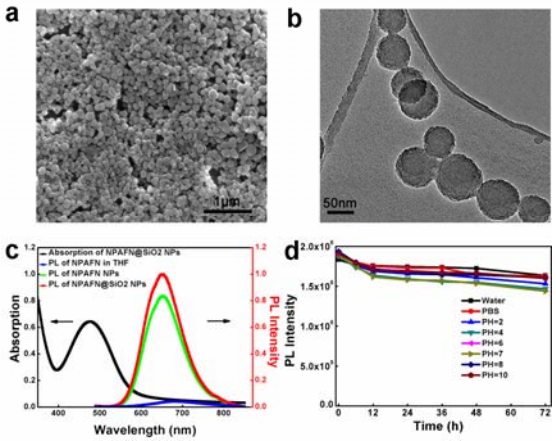

Fig. 1. (a), (b) SEM and TEM image of NPAFN@SiO_2 NPs (c) Absorption of NPAFN@SiO_2 NPs and fluorescence spectra of NPAFN in THF solution, NPAFN NPs and NPAFN@SiO_2 NPs; (d) Fluorescence stability of modified NPAFN@SiO_2 NPs in different conditions;

The synthetic protocol is shown in Fig. S1a. NIR dye 2,3-bis(4'-(diphenylamino)-[1,1'-biphenyl]-4-yl) fumaronitrile (NPAFN) were first prepared into NPs.[6] Scanning electron microscopy (SEM) image (Fig. S1b) indicates the NPAFN NPs have roughly spherical structures with an average diameter of about 90 nm. Then, the as-prepared NPAFN NPs were coated with a thin layer of silica shell (see experimental section 1.5). Compared to the smooth surface of the nude NPs (Fig. S1c), the NPAFN@SiO_2 NPs show rather rough surface (Fig. 1b). Since the contrast between organic NPs and silica shell was low, no obvious core-shell structure was observed as expected. EDX analysis further confirmed the existence of silicon (Fig. S2). The average hydrodynamic diameter of NPAFN@SiO_2 NPs determined by DLS was approximately 110 nm (Fig. S3).

After the successful coating of silica shell on the NPAFN NPs, the optical properties were then investigated. It should be noted that NPs exhibit intense NIR fluorescence with emission peak at 650 nm, which would have deeper penetration into biological tissues and reduce optical interference like autofluorescence and light scattering. In addition, the NPAFN@SiO_2 NPs show similar

absorption and emission band as that of NPAFN NPs, due to the thin transparent and insulating silica nanoshell (Fig. 1c). Notably, the fluorescence QY of NPAFN@SiO_2 NPs was measured to be much higher than that of NPAFN NPs (see experimental section 1.6). The enhanced emission property was possibly attributed to the following reasons. Firstly, the initial NPAFN NPs has the typical characteristic of AIEE, coating with a thin layer of silica nanoshell outside the NPs would make much closer aggregation of molecules in the NPs and thus further blocks the non-radiative path and activates the radiative decay for the fluorescence enhancement.[7] Secondly, with the protection of the inert silica nanoshell, the NPs can be isolated from the external environment, which will effectively prevent unexpected quenching of the outer NPAFN molecules by the external surface adsorbates or redoxactive molecules. In addition, the possibility of the leakage of dye molecules from the NPs can be largely restrained as well. The Stokes shift of the NPs is as large as 175 nm, which would increase the signal-to-background ratios (sensitivity) via reducing the autofluorescence of the bio-substrate and interferences between excitation and emission. All these features endow the NPs with superior advantages as a potential probe especially for high sensitive in vivo imaging at a low concentration.

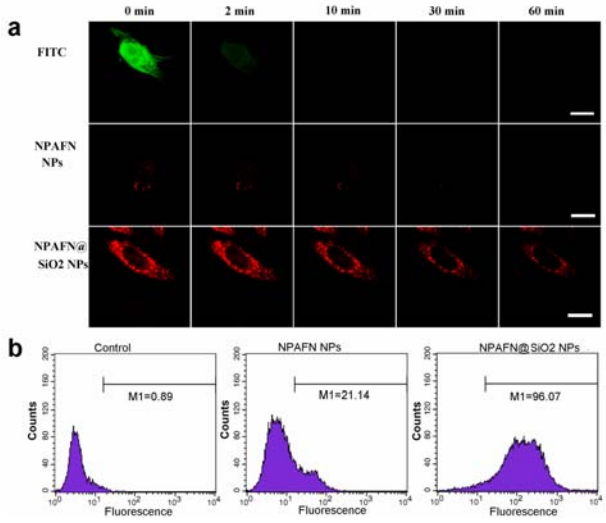

Fig. 2. (a) Stability comparison of fluorescence signals of KB cells imaged by FITC, NPAFN NPs and NPAFN@SiO_2 NPs in the same concentration respectively. Scale bars: 10 μm; (b) Fluorescent intensity of NPAFN NPs and NPAFN@SiO_2 NPs at the same concentration in cells analyzed by fluorescene-activated cell sorting (FACS), PBS was used as control group.

To improve the water-dispersibility and bio-environmental stability of NPAFN@SiO_2 NPs, we used amphipathic surfactant C18PMH-PEG, an effective biocompatible building block that has been widely used in bio-applications, to make further surface functionalization.[8] The functionalized NPs experienced a slight increase in size (Fig. S3). As shown in Fig. S4a and 1d, the NPAFN@SiO_2 NPs preserve very stable size and fluorescence over wide pH range of 2-10 even after 72 h, and no obvious changes could be detected in different bio-environments. Such great improvement of bio-environmental stability would make in vitro and in vivo imaging possible. To estimate the potential cytotoxicity of NPAFN@SiO_2 NPs, we measured the viability of three different cell lines including KB cells, A549 cells and 4T1 cells by using the standard 3-(4,5-dimetylthiazol-2-yl)-2,5-diphenyltetrazolium bromide (MTT) assay. All these three kinds of cells exhibited low cytotoxicity with high cell viability (>85%) after 24 h incubation with NPAFN@SiO_2 NPs of different concentrations from 5 to 20 μM as shown in Fig. S4b, indicating that the NPs had little interference with the cell physiology and proliferation.

Although organic dyes have been widely used as fluorescent labels for bioimaging, the low photostability significantly limits their practical applications for long-term bioimaging. As such, we further compared the photostability of the NPAFN NPs and NPAFN@SiO_2 NPs with fluorescein isothiocyanate dye (FITC), which is one of the most stable organic dyes commonly used in bioimaging, under 488 nm laser illumination. The fluorescence of FITC rapidly diminished and became negligible after 2 minutes, due to severe photo-bleaching (Fig. 2a). In a sharp contrast, the fluorescence signals of NPAFN@SiO_2 NPs preserve a strikingly stable fluorescence, and could maintain distinctive red fluorescence even after 60 min irradiation. When the KB cells are labeled with the same concentration of NPAFN NPs and NPAFN@SiO_2 NPs, it is also revealed that the NPAFN@SiO_2 NPs maintained more superior photostability than that of NPAFN NPs (Fig. 2a and S4c). More importantly, the NPAFN@SiO_2 NPs are observed to exhibit strikingly brighter fluorescence than that of NPAFN NPs under the same incubation concentration. Although the QY of NPAFN@SiO_2 NPs is already confirmed to be higher than that of NPAFN NPs, the reason for the remarkable fluorescence enhancement is still not completely clear. As such, we further carried out flow cytometry to evaluate the cellular uptake of NPAFN NPs and NPAFN@SiO_2 NPs under the same incubation concentration (Fig. 2b). It is found that the fluorescence intensity of NPAFN@SiO_2 NPs was five times higher than that of NPAFN NPs, indicating that silica shell coated NPs are more easily internalized by cells possibly due to the better membrane-penetrating capacity induced by their rough surface as well as their much favorable biocompatibility.[9] The noted brightness and remarkable photostability make the red-emitting NPAFN@SiO_2 NPs a promising excellent probe for applications in long-term and real-time bioimaging.

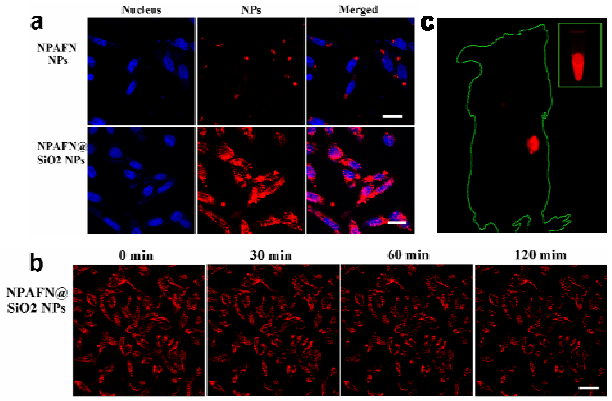

Fig. 3. (a) Confocal laser-scanning fluorescent microscopy images of KB cells incubated with NPAFN NPs and NPAFN@SiO_2 NPs; Scale bars: 20 μm. (b) Temporal

fluorescence evolution of the KB cells labeled with NPAFN@SiO_2 NPs. Scale bar: 40 μm, excitation wavelength was 488 nm. (c) In vivo fluorescence image of the mice at 12 h after injection of the NPAFN@SiO_2 NPs. Inset is the fluorescence image of NPs in the storage equipment.

The biocompatible, highly photo- and pH-stable, ultra-bright NIR fluorescent NPAFN@SiO_2 NPs are further explored as biological fluorescent probes for in vitro imaging. Fig. 3a shows images of the KB cells imaged with NPAFN NPs and NPAFN@SiO_2 NPs in the same concentration, both stained with DAPI. The fluorescence of NPAFN@SiO_2 NPs labeled KB cells was observed to be particularly bright compared to that of NPAFN NPs at the same concentration, in good accord with the photostability study and cellular uptake result determined by FACS (Fig. 2b). Based on the high photostability and excellent biocompatibility of the resultant NPAFN@SiO_2 NPs, we further verify the possibility of utilizing it as fluorescent probe for long-term imaging. As shown in Fig. 3b, even after 120 min continuous irradiation, the NPAFN@SiO_2 NPs preserved a strikingly stable fluorescence due to the robust photostability, which is particularly suitable for long-term imaging.

The NPAFN@SiO_2 NPs level in the blood was first studied over time. A blood circulation half-life of 2.5 h was observed for NPAFN@SiO_2 NPs as shown in Fig. S5. The NPAFN@SiO_2 NPs were then intravenously injected into 4T1 tumor-bearing BALB/c mice for in vivo imaging, hair of the mice were removed from neck to foot. With time went by, accumulation of the NPs in the tumor site with intense fluorescence was observed. Significantly, even with the exposure time was reduced to 15 ms, after 12 hours post injection the fluorescent signals of NPAFN@SiO_2 NPs were still distinctively bright and highly spatially resolved, in sharp contrast to extremely low signals in other parts of the mouse body even in the hair, which show strong autofluorescence before injection (Fig. S6). And almost no autofluorescence background detected, as shown in Fig. 3c. Such high signal to noise ratio (sensitivity) is particularly beneficial for NIR probes for cancer diagnosis. We then studied the biodistribution of the NPs by imaging the major organs and the tumor tissues of 4T1 tumor-bearing BALB/c mouse at different post injection time points (Fig. S7). Consistent with the in vivo imaging results, the fluorescence of NPs in the tumor tissues increased with time. After 24 h post injection, prominent accumulation of NPs in tumor sites were observed (41.1% ID g-1), which were higher than that in liver (32.5% ID g-1). Those studies clearly evidenced the advantages of the NPAFN@SiO_2 NPs for in vivo imaging.

The in vivo toxicity assessment of the NPAFN@SiO_2 NPs was also evaluated, which is mainly assessed from the loss of body weight, hematology analysis, and blood biochemical assay. No statistically significant weight loss, histopathological abnormities, hepatic and kidney disorder were observed in the treatment groups compared with control group (Fig. S8, S9). These data indicated a negligible in vivo toxicity for NPAFN@SiO_2 NPs as biocompatible fluorescence probe for bioimaging.

Conclusions

We have demonstrated a novel silica-coated dye NP to achieve highly luminescent and ultraphotostable NIR fluorescent probes for in vitro and in vivo imaging. Much higher brightness with enhanced QY and much more superior photostability were observed for silica-coated NPs than that of uncoated NPs. Application of core-shell NPs for in vitro and in vivo imaging was also demonstrated respectively. Systematic in vivo toxicity study also indicated the biocompatibility of the NPAFN@SiO_2 NPs. This work highlights the great potential of the silica-coated dye NPs for high efficient in vitro and in vivo bioimaging.

This work was supported by National Basic Research Program of China (973 Program, Grant Nos. 2013CB933500, 2012CB932400, 2011CB808400), and National Natural Science Foundation of China (Nos. 51173124, 51172151). X. J. Hao and M. J. Zhou contribute equally to this work.

Notes and references

[a] *Functional Nano & Soft Materials Laboratory (FUNSOM) and Jiangsu Key Laboratory for Carbon-Based Functional Materials & Devices, Soochow University, Suzhou, Jiangsu 215123, China; Tel: 86 512 65889855; E-mail: xjzhang@suda.edu.cn; jsjie@suda.edu.cn*
[b] *Nano-organic Photoelectronic Laboratory and Key Laboratory of Photochemical Conversion and Optoelectronic Materials, Technical Institute of Physics and Chemistry, Chinese Academy of Sciences, Beijing 100190, China; Tel: 86 010 82543510; E-mail: xhzhang@mail.ipc.ac.cn*

† Electronic Supplementary Information (ESI) available: [details of any supplementary information available should be included here]. See DOI:10.1039/b000000x/

1 (a) V. Ntziachristos, *Nat. Meth.*, 2010, **7**, 603-614. (b) X. Gao, Y. Cui, R. M. Levenson, L. W. Chung and S. M. Nie, *Nat. Biotech.*, 2004, **22**, 969-976.
2 (a) N. Li, C. Chang, W. Pan, B. Tang, *Angew. Chem. Int. Ed.*, 2012, **51**, 7426-7430. (b) R. Bardhan, S. Lal, A. Joshi and N. J. Halas, *Acc. Chem. Res.*, 2011, **44**, 936-946.
3 (a) B-K. An, S-K. Kwon, S-D. Jung and S. Y. Park, *J. Am. Chem. Soc.*, 2002, **124**, 14410-14415. (b) H. Z. Wu, T. S. Yang, Q. Zhao, J. Zhou, C. Y. Li and F. Y. Li, *Dalton Trans.*, 2011, **40**, 1969-1976.
4 Y. L. Yang, F. F. An, Z. Liu, X. J. Zhang, M. J. Zhou, W. Li, X. J. Hao, C. S. Lee, X. H. Zhang, *Biomaterials*, 2012, **33**, 7803-7809.
5 (a) J. H. Park, L. Gu, G. von Maltzahn, E. Ruoslahti, S. N. Bhatia, M. J. Sailor, *Nat. Mater.*, 2009, **8**, 331-336. (b) Q. Liu, T. S. Yang, W. Feng and F. Y. Li, *J. Am. Chem. Soc.*, 2012, **134**, 5390-5397. (c) D. P. Ferris, J. Lu, C. Gothard, R. Yanes, C. R. Thomas, J-C. Olsen, J. F. Stoddart, F. Tamanoi, J. I. Zink, *Small*, 2010, **7**, 1816-1826. (d) L. S. Wang, L. C. Wu, S. Y. Lu, L. L. Chang, I. T. Teng, C. M. Yang and J. A. Ho, *ACS Nano*, 2010, **4**, 4371-4379.
6 X. Diao, W. Li, J. Yu, X. J. Wang, X. J. Zhang, Y. L. Yang, F. F. An, Z. Liu and X. H. Zhang, *Nanoscale*, 2012, **4**, 5373-5377.
7 (a) S. Kim, T. Y. Ohulchanskyy, H. E. Pudavar, R. K. Pandey, P. N. Prasad, *J. Am. Chem. Soc.*, 2007, **129**, 2669-2675. (b)Y. Hong, J. W. Lam, B. Z. Tang, *Chem. Commun.*, 2009, **29**, 4332-4353.
8 (a) W. Li, Y. L. Yang, C. Wang, Z. Liu, X. J. Zhang, F. F. An, X. J. Diao, X. J. Hao and X. H. Zhang, *Chem. Commun.*, 2012, **48**, 8120-8122. (b) M. J. Zhou, X. J. Zhang, Y. L. Yang, Z. Liu, B. S. Tian, J. S. Jie and X. H. Zhang, *Biomaterials* 2013, **34**, 8960.
9 I. I. Slowing, B. G. Trewyn, S. Giri, V. Y. Lin, *Adv. Funct. Mater.*, 2007, **17**, 1225-1236.